FLOW OVER INCLINED BODIES[1]

By E. W. Perkins and F. E. Gowen
Ames Aeronautical Laboratory

There are available at present several theoretical methods for predicting the aerodynamic characteristics of slender inclined bodies of revolution. Most of these methods are based upon potential-flow solutions and employ perturbation methods and thus suffer from two very serious limitations. First, these theories predict only initial lift-curve slopes and are therefore useful in only the very low angle-of-attack range. Second, and perhaps most important, since the theories are potential-flow solutions they fail to consider any effects of viscosity.

It has been generally observed by experimenters that the lift-curve slope of an inclined body of revolution increases with increasing angle of attack. An extension of slender-body theory by Lighthill (reference 1) includes terms in the square and cube of the angle of attack; however, the contributions of these terms at moderate Mach numbers are, in general, insufficient to account for the nonlinearity observed in the experimental data.

It has long been recognized that the effects of viscosity have an important influence on the flow over inclined bodies of revolution. Allen (reference 2) has developed a semiempirical method for calculating these effects for slender bodies as illustrated in figure 1. It has been shown that the component of velocity normal to the inclined body axis $V_o \sin \alpha$, which results in no net force in a potential flow, contributes important forces in the cross-flow direction in a viscous fluid. These forces result from the separation of the cross flow on the lee side of the body. Thus, this so-called viscous cross force results from much the same type of flow as occurs for a circular cylinder in two-dimensional flow. Hence, in Allen's analysis the effects of viscosity on the local cross force are related to the drag of an element of a circular cylinder in two-dimensional flow. As illustrated in figure 1, one of the basic assumptions of the method is that this viscous cross force may be simply combined with a potential cross force in the calculations of the total local cross force f. In this expression q is the dynamic pressure; ds/dx is the rate of change of body-cross-section area with distance along the body; C_{d_c} is the section drag coefficient of a circular cylinder of the same local radius r at a Reynolds number and Mach number based upon the cross component of velocity; and η is a factor to allow for the decrease in section drag coefficient due to the finite length of the body. The dashed curve in figure 1 shows the potential contribution to the cross-force distribution;

[1]This is a reprint of the paper by the same authors which was presented at the NACA Conference on Aerodynamic Design Problems of Supersonic Guided Missiles at the Ames Aeronautical Laboratory on Oct. 2-3, 1951.

whereas, the solid curve includes the allowance for viscous effects. Based upon this distribution of local cross force the lift, the drag-rise, and the pitching-moment characteristics of inclined bodies may be calculated. A typical example of the comparison between experiment and theory is shown in figure 2. It is apparent that the potential theory alone is inadequate in all but the very low angle range where the viscous effects are very small.

Comparison of the result of Allen's approximate theory with the experimental force and moment characteristics for a wide variety of bodies over a large Mach number range (reference 3) showed that this simple allowance for viscous effects yields results for the lift and drag increment which are in fair agreement with experiment. However, it was noted, in general, that the center-of-pressure position was more rearward by approximately 1 body diameter than the theory predicted.

Perfect agreement with experiment would not be expected since the potential theory used applies only for very slender bodies and the viscous contribution would be expected to be exact only at stations far downstream from the nose of the body.

The results of visual flow and pressure distribution studies (reference 3) have demonstrated the similarity between the cross flow for an inclined body of revolution and the two-dimensional flow about a circular cylinder. It has been shown that the circumferential pressure distributions for the inclined body and the circular cylinder deviate from their respective theoretical inviscid distributions on the lee or downstream side in much the same manner. With the aid of a visual flow technique, it has been shown that there is a shedding of vortices within the cross-flow field of the inclined body. However, unlike the phenomenon associated with the circular cylinder, the shedding from the inclined body is not periodic. It has also been found that the vortex configuration depends to a large extent on the shape of the nose of the body.

To illustrate these effects better, vapor-screen pictures were made with the aid of the experimental setup shown in figure 3. A camera is mounted within the wind tunnel on the model support strut downstream from the model. The camera "looks" upstream and is focused on the plane of the vapor screen. The approximate field of view of the camera has been indicated. It has been generally observed that there is a stable symmetric vortex pair associated with a lifting body at low angles of attack. As the angle of attack is increased, the vortex configuration becomes asymmetric and aperiodically unsteady. Typical results obtained for a body with an ogival nose and a body with a sharp conical nose are shown in figure 4. These vapor-screen pictures show that the vortex configuration associated with the ogival-nosed body remain symmetric to a much higher angle of attack than did the configuration for the body

with the sharp conical nose. For both models in the high angle-of-attack range, the vortex configuration was asymmetric and unsteady. The unsteadiness of the flow was associated with an aperiodic switching of the vortices from side to side as illustrated in figure 5. The data in figure 5 are sequences taken from a movie which shows the change in the vortex configuration with time at two angles of attack for the model with the ogival nose. These pictures were taken at 10 frames per second and indicate the rapidity with which the vortex configuration changes in the high angle-of-attack range. The results of these vapor-screen studies show that the cross-flow wake for the ogival-nosed body is not only symmetric but is also steady to a much higher angle of attack than is the cross-flow wake for the model with the sharp conical nose.

The unsteady nature of the flow in the cross-flow wake of the inclined bodies at large angles of attack would be expected to result in erratic fluctuations in the rolling moment and side force for a missile configuration with aft surfaces which were immersed in the cross-flow wake from the lifting forebody. Since these erratic characteristics are undesirable, it is evident that of the two nose shapes for which information was presented the ogival nose had the better characteristics. The results of additional studies made with the vapor-screen technique have shown that, from the standpoint of avoiding the problems associated with the asymmetry and unsteadiness in the cross-flow wake, slender pointed nose shapes similar to the conical nose should be avoided.

Although the vapor-screen pictures serve as an indication of the presence of vortices in the cross-flow field they yield only qualitative information. To provide a quantitative measure of the flow conditions in the vicinity of the vortices, downwash measurements have been made in the plane of the base of the model. A vapor-screen photograph and the corresponding downwash distribution along a line 1.4 body radii above the body axis are shown in figure 6. At this angle of attack the vapor-screen photograph for this model with the tangent ogive nose indicates the presence of a symmetric pair of vortices on the lee side of the body and, as anticipated, the downwash measurements show a distribution characteristic of two symmetrically disposed vortices.

As was noted from figure 4, as the angle of attack was increased the vortex configuration changed from the symmetric pair to an asymmetric configuration. It has been observed that the asymmetric configuration remained steady at certain angles of attack, whereas with small changes in angle the configuration may become unsteady. Figure 7 shows a vapor-screen picture of a steady asymmetric vortex configuration and the corresponding variation of downwash along a line approximately 3 body diameters above the body center line. The stream-angle distribution is asymmetric as would be expected from the vapor-screen picture.

[redacted]

It appears from vapor-screen studies that the fluctuations of flow were of an aperiodic nature. However, more conclusive evidence of the aperiodicity was obtained from time histories of the static pressure fluctuations on the body. In figure 8 is shown the surface-pressure fluctuation obtained with the aid of a capacitance-type pressure cell located at the position indicated on the sketch. Although the data presented cover only a relatively short time interval, it is apparent that the pressure fluctuations are aperiodic and of varying amplitude. For the data presented, the pressure cell was at the approximate circumferential location of the vortex core. At this position and angle of attack the magnitude of the pressure fluctuations was most severe. The maximum pressure fluctuations at lower angles of attack and at other circumferential positions were of the order of one-quarter of this magnitude.

For any missile which must operate at large angles of attack and for which the tail surfaces are immersed in the vortex flow field on the lee side of the body, the asymmetric and unsteady nature of this flow will promote unexpected and erratic rolling as well as undesirable forces and moments in yaw. Although these forces in themselves may not be important, the continual fluctuation of the forces would tend to expend an intolerable amount of the available control fluid.

Wind-tunnel tests have been conducted on a number of models to determine the magnitude and frequency characteristics of the fluctuating forces. Time histories of the side force and rolling moments were obtained with the aid of a multiple-channel recording galvanometer. A series of sections from typical records are presented in figure 9. The records indicate the variation with time of the rolling and side forces at several angles of attack for the model shown schematically at the top of the figure. The records show that at 25.5° angle of attack this symmetric model was subject to a large rolling force resulting from the asymmetry of the flow in the cross-flow wake from the body. In addition to this force, which results in an average rolling-moment coefficient of approximately 0.05 based on the total area and span of the tail fin, there is a fluctuating moment resulting from the unsteadiness of the vortex flow from the forebody. With a change in angle of attack from 25.5° to 27° the average rolling moment reversed sign although the fluctuations were of about the same magnitude. With further increases in angle of attack to 28.6°, the model suffered violent fluctuations in both roll and side force. This condition corresponds to the angle of attack at which very rapid switching of the vortices from side to side was observed in the vapor-screen studies. A further increase in angle of attack resulted in another reversal in the sign of the average rolling force and a large diminution of the fluctuations.

The results of testing this model with the sharp conical nose throughout the angle-of-attack range to a maximum of approximately 34°

are shown in figure 10. On the upper graph is plotted the average rolling moment at each angle of attack; whereas in the lower graph is plotted the magnitude of the maximum fluctuation of the rolling moment. It is evident from the upper graph that the average rolling moment was small until the angle of attack exceeded approximately 23°. Above 23° the asymmetric flow resulted in large rolling forces which varied rapidly with angle of attack. At angles as low as 10° some fluctuations in roll were exhibited by the model with the sharp conical nose. The maximum value of the fluctuating rolling moment occurred at approximately 30° angle of attack. With further increase in angle of attack above 30°, the fluctuating forces diminished. A better appreciation of the control problem involved is obtained if one realizes that the maximum indicated roll coefficient is that which would be developed by approximately a 12° deflection of the tail fin.

Data for a similar model with an ogival nose are shown in figure 11. Comparison of these data with the results for the conical-nosed body show that, although the average rolling moment due to the flow asymmetry is of the same order of magnitude, the variation with angle of attack was not nearly so erratic. For this model, the fluctuating component of roll is negligibly small to an angle of attack of about 18° and the maximum value of the fluctuating roll was only approximately half that of the model with the conical nose. These results are in general agreement with the indications of the vapor-screen tests where it was observed that, for the model with the ogive nose, the flow in the cross-flow wake was steady and the vortex configuration symmetric to higher angles of attack than for the model with the sharp conical nose.

Shown in figure 12 are the results of some preliminary tests conducted in the Ames 6- by 6-foot supersonic tunnel on a model of somewhat higher fineness ratio. The magnitudes of the rolling-moment coefficient are not given since some question remains as to the interpretation of the records obtained because of the dynamic characteristics of the model and support system. Nevertheless, the trends with increasing angle of attack and Mach number are clearly evident. The data show the variation of the fluctuating rolling moment with angle of attack for several Mach numbers. The variation with angle of attack is qualitatively the same at each of the supersonic Mach numbers and in general indicates a decrease in magnitude with increasing Mach number. The tests at a Mach number of 0.9 were terminated at 20° angle of attack because of the violent oscillations of the model.

The results of recent vapor-screen studies of several bodies in the Ames 1- by 3-foot supersonic tunnel have indicated that an increase in Reynolds number tends to reduce the angle of attack at which unsteadiness in the cross flow occurs. However, no direct correlation with Reynolds number has been found.

It has been shown in a preceding paper by Seiff and Sandahl that the use of blunt-nosed shapes is desirable from a standpoint of drag reduction. The vapor-screen studies have shown that in addition to yielding a drag reduction the use of blunt-nosed shapes is beneficial in that an increase in the angle of attack at which unsteadiness in the cross-flow wake occurs is realized.

It is apparent that only general trends may be deduced from the results of the wind-tunnel tests since in these tests the models were rigidly mounted on a balance system which restricted their movement. It does not appear unreasonable to expect that for missiles in free flight there could be an aerodynamic coupling between the motion of the body and the shedding of the vortices such that a periodic oscillation might result. Tests which are presently being conducted by the free-fall technique should yield some information on the effects of the vortex discharge on the free-flight characteristics of a missile-like configuration.

It has been shown that the effects of viscosity on the flow over inclined bodies of revolution are important and must be considered in the calculation of the forces and moments at any appreciable angle of attack. As a result of the asymmetry and unsteadiness of the flow in the cross-flow wake from an inclined body, fluctuations in roll and side force occur for a missile-like body-tail combination at large angles of attack. The results of wind-tunnel tests have shown that the use of blunt-nosed shapes tends to alleviate the problem somewhat by increasing the useful angle-of-attack range and by reducing the magnitude of the unsteady rolling forces.

REFERENCES

1. Lighthill, M. J.: Supersonic Flow past Slender Pointed Bodies of Revolution at Yaw. Quarterly Jour. Mech. and Appl. Math., vol. 1, pt. 1, March 1948, pp. 76-89.

2. Allen, H. Julian: Estimation of the Forces and Moments Acting on Inclined Bodies of Revolution of High Fineness Ratio. NACA RM A9I26, 1949.

3. Allen, H. Julian, and Perkins, Edward W.: Characteristics of Flow over Inclined Bodies of Revolution. NACA RM A50L07, 1951.

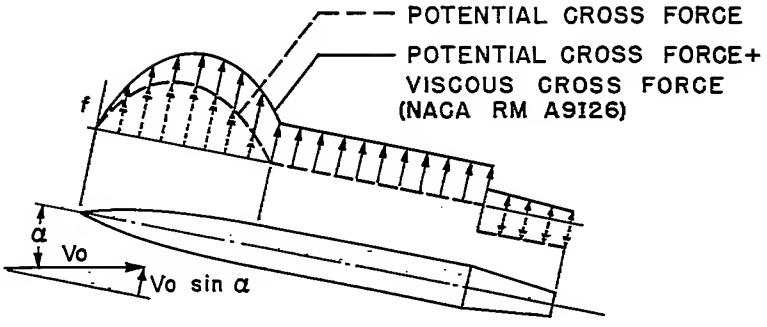

$$f = \begin{matrix}\text{POTENTIAL} \\ \text{CROSS FORCE}\end{matrix} + \text{VISCOUS CROSS FORCE}$$

$$= 2q\left(\frac{ds}{dx}\right)\alpha + 2\eta\, C_{d_c}\, q\, r\alpha^2$$

Figure 1.- Schematic diagram of cross-force distribution.

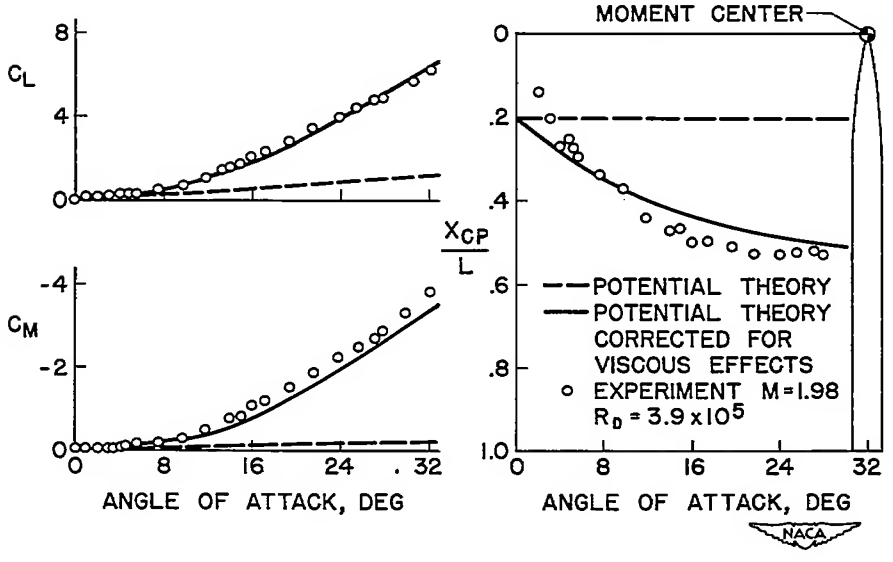

Figure 2.- Typical comparison of experiment and theory.

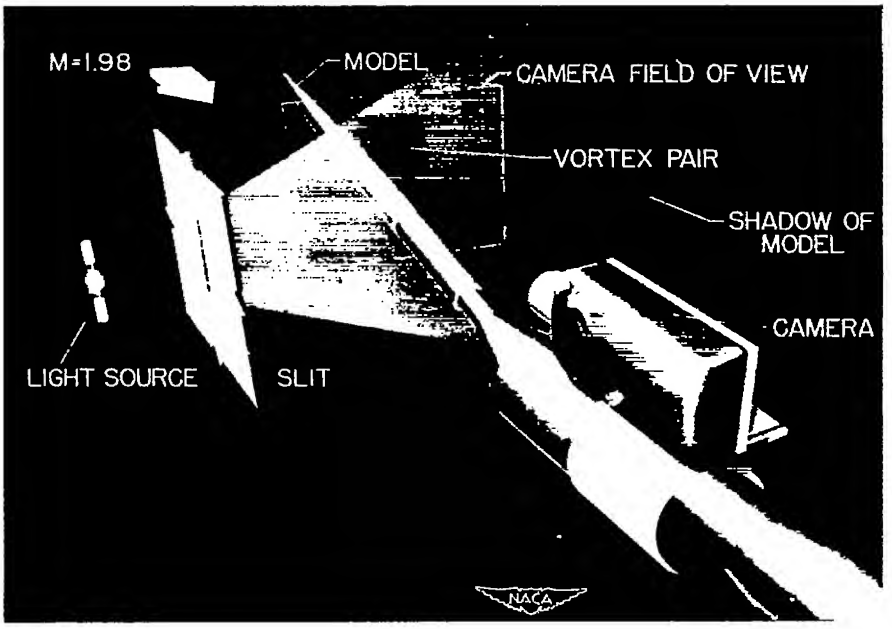

Figure 3.- Schematic diagram showing orientation of camera and model for vapor-screen tests.

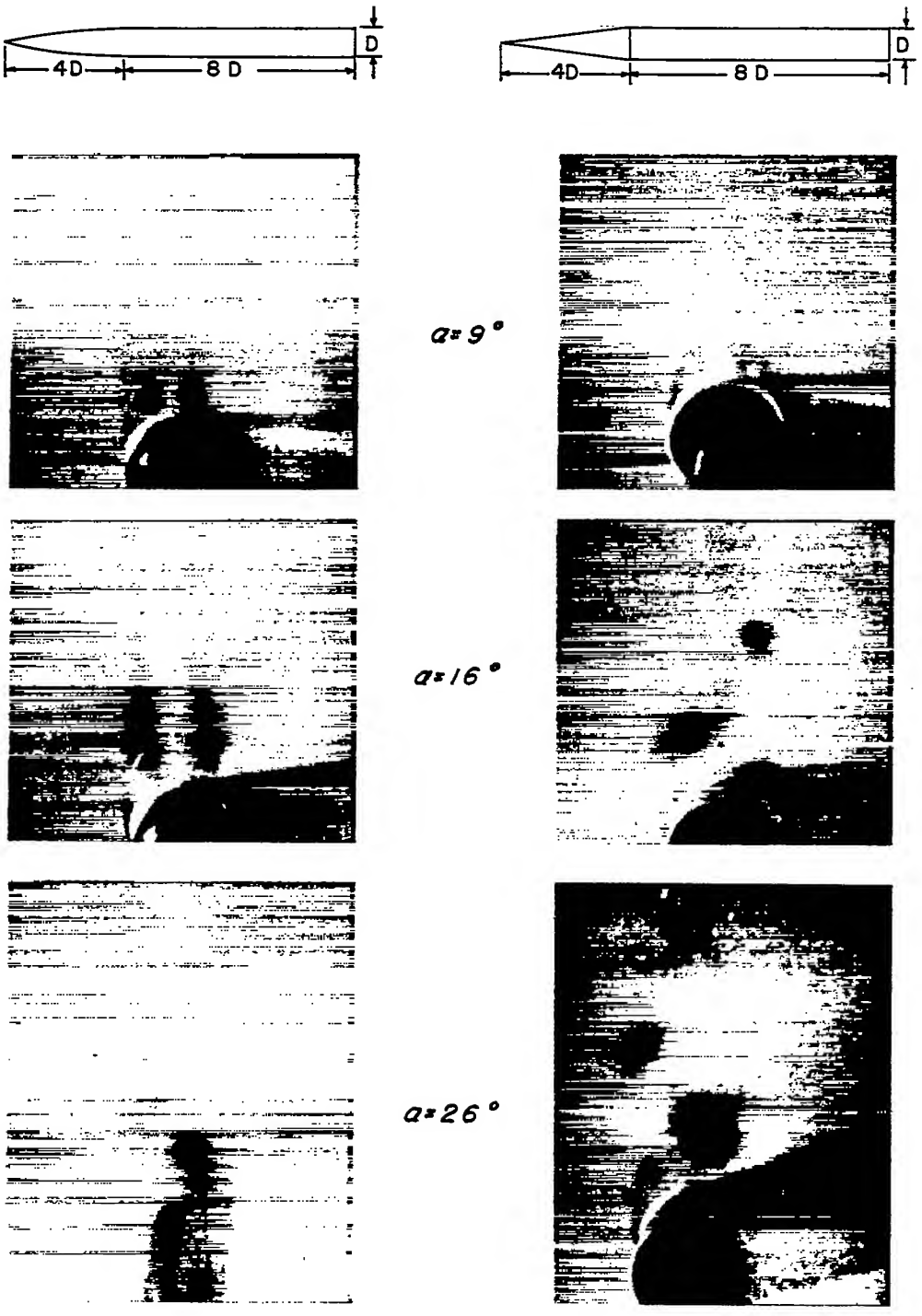

Figure 4.- Effect of nose shape on the variation with angle of attack of the vortex configuration.

NACA

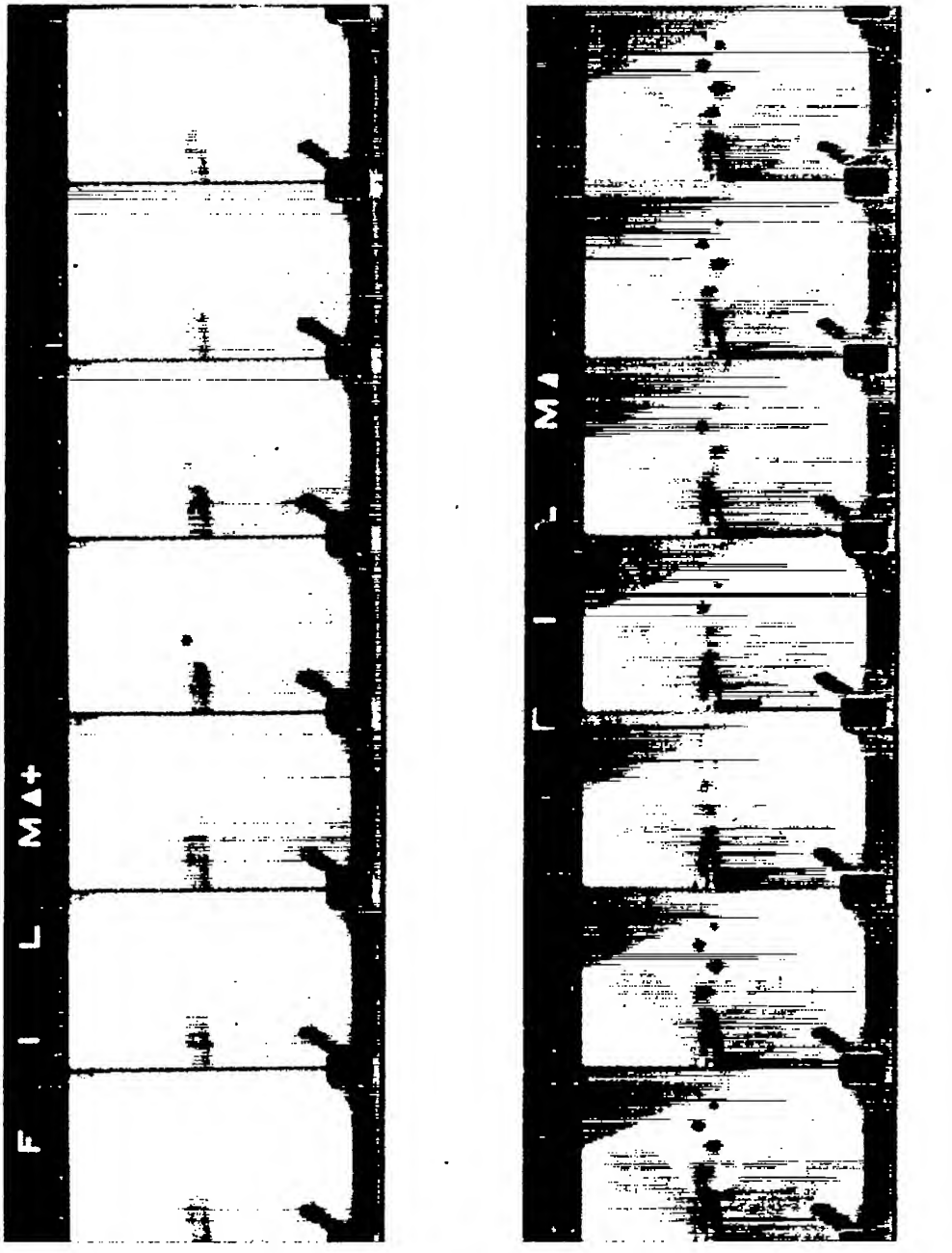

Figure 5.- Vapor-screen pictures showing fluctuation of the vortices in the cross-flow wake of the body with the ogival nose.

[redacted]

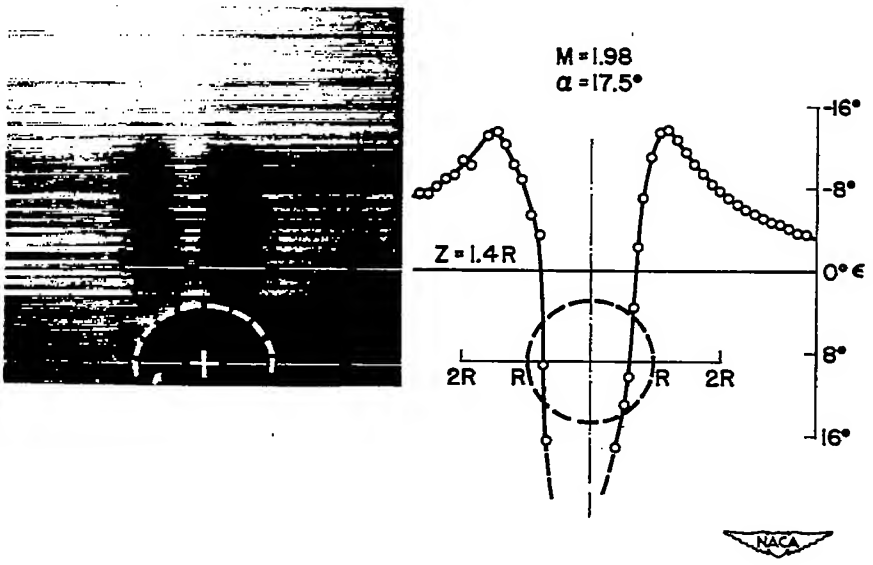

Figure 6.- Downwash distribution through vortex pair.

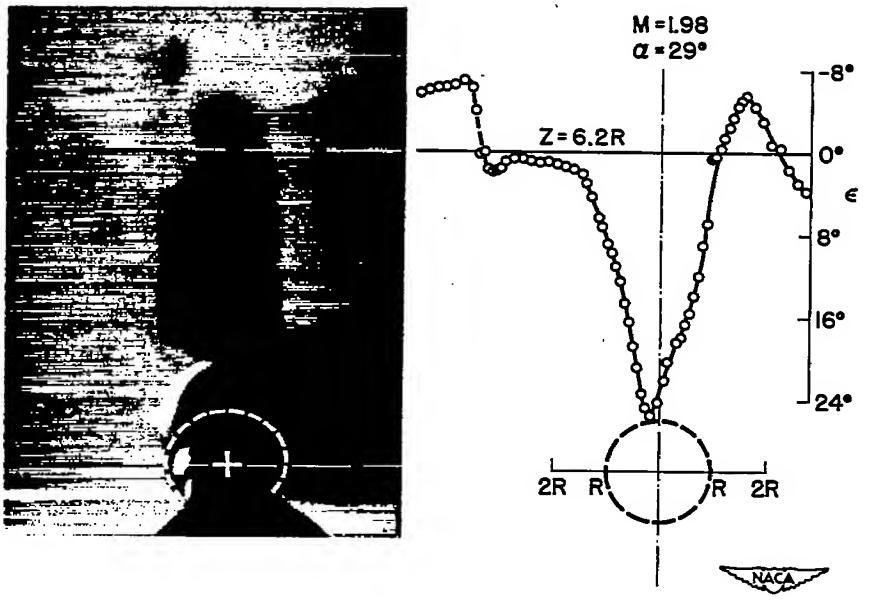

Figure 7.- Downwash distribution through asymmetric vortex configuration.

[redacted]

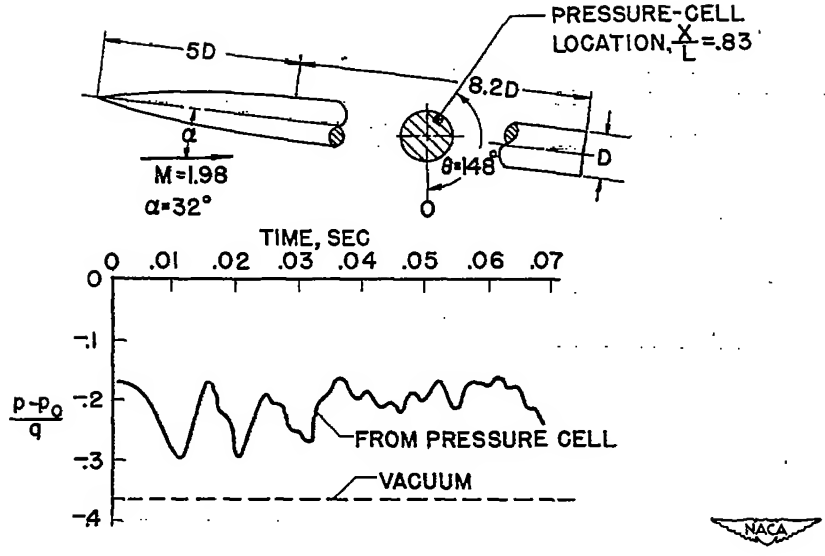

Figure 8.- Surface-pressure fluctuations accompanying unsteady flow in the cross-flow wake.

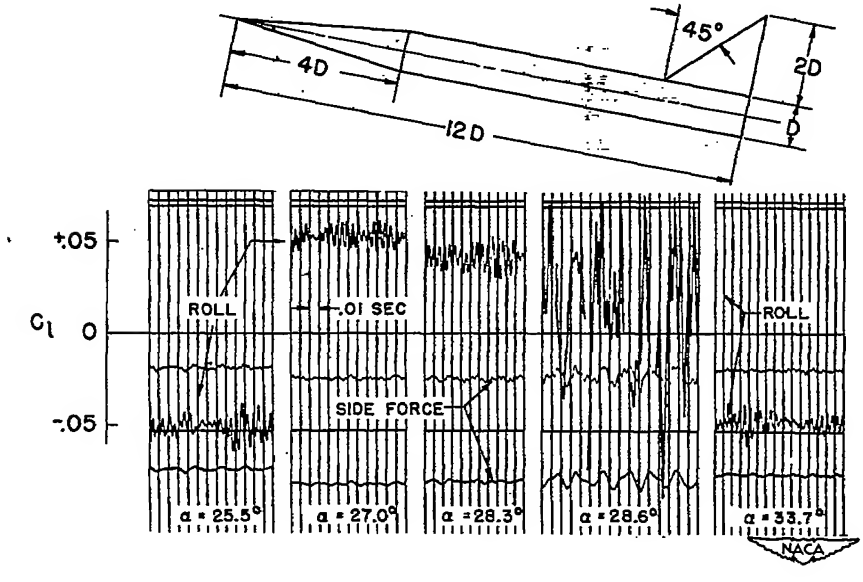

Figure 9.- Typical oscillograph records of roll and side force fluctuations.

[redacted]

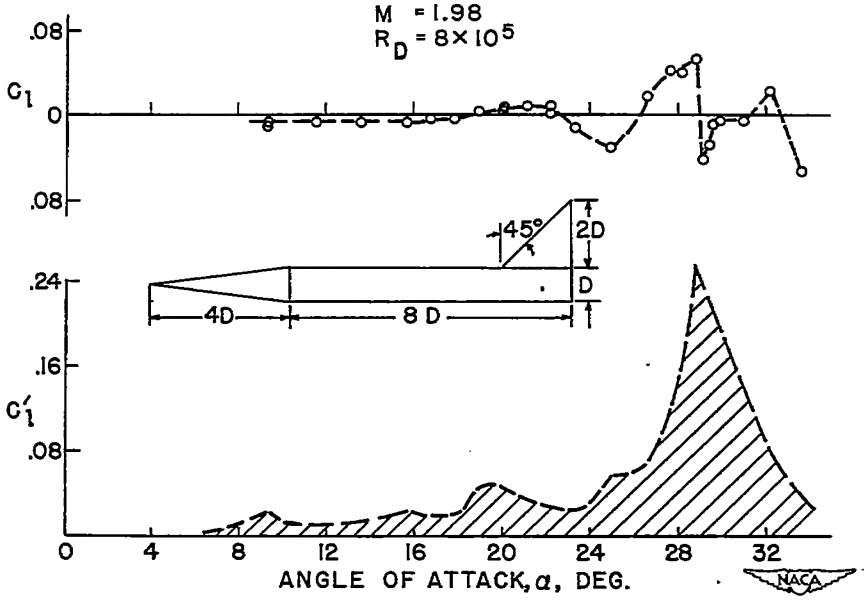

Figure 10.- Variation of the average rolling-moment coefficient and the maximum fluctuating rolling-moment coefficient for a body-tail combination with conical nose.

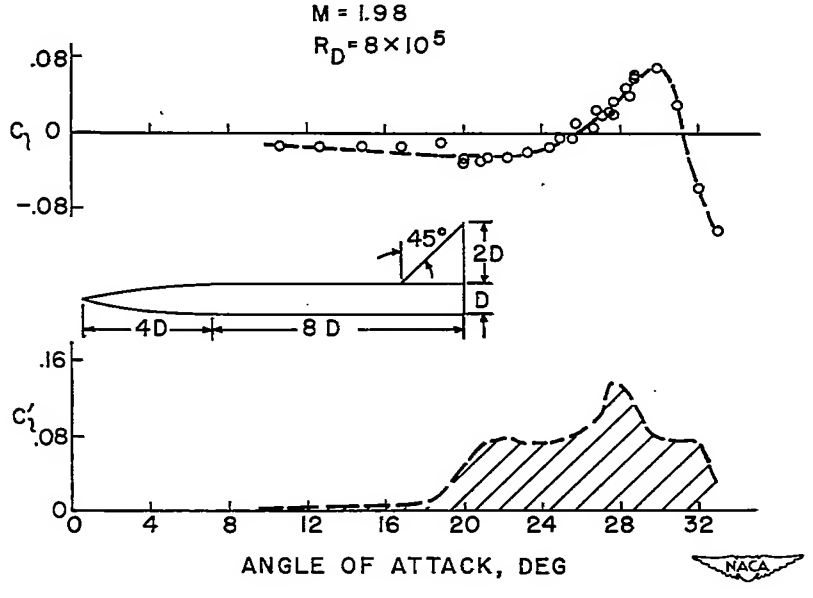

Figure 11.- Variation of the average rolling-moment coefficient and the maximum fluctuating rolling-moment coefficient for a body-tail combination with ogival nose.

[redacted]

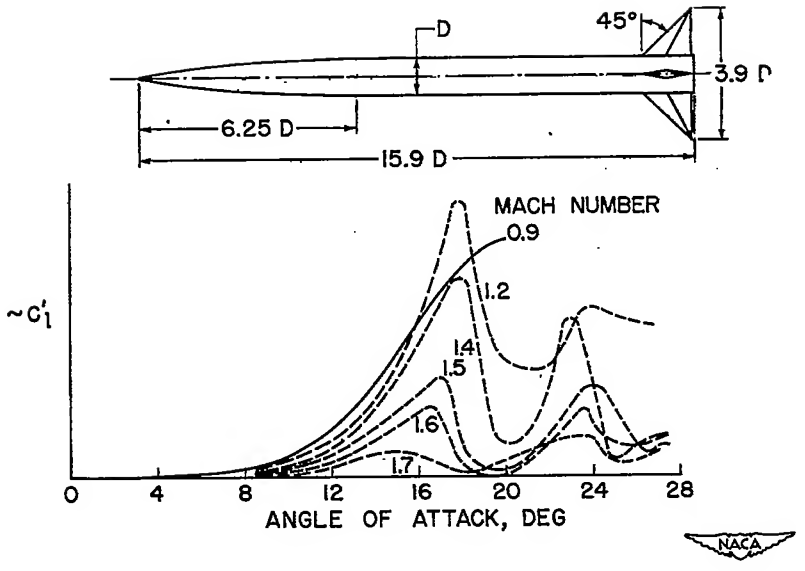

Figure 12.- Effect of Mach number on the maximum amplitude of the fluctuating rolling moment.

NACA-Langley - 11-9-51 - 325